ELSEVIER

Thermochimica Acta 314 (1998) 111–121

thermochimica acta

Heat capacity of liquid Al–La–Ni alloys

J. Schmid, F. Sommer*

Max-Planck-Institut für Metallforschung and Institut für Metallkunde der Universität Stuttgart, Seestr. 75, D-70174 Stuttgart, Germany

Received 15 September 1997; accepted 1 October 1997

Abstract

The heat capacity of liquid Al–La–Ni alloys was measured using an adiabatic calorimeter. The heat capacities $C_p(x,T)$ exhibit large temperature and composition dependences. The results indicate the existence of a maximum in the $C_p(T)$-curve in the undercooled melt. An association model was applied to calculate the thermodynamic mixing functions of ternary liquid Al–La–Ni alloys using the model parameters of the three limiting binary systems and assuming an additional ternary association reaction. The calculations show a good agreement with the experimental enthalpy of mixing and the $C_p(x,T)$- data.

Keywords: Adiabatic calorimeter; Al–La–Ni; Association model; Heat capacity

1. Introduction

Ternary Al–La–Ni alloys are known for their good glass-forming ability by rapid quenching from the liquid state [1] and for their ability for hydrogen storage in the solid state [2]. The glass-forming ability of liquid alloys is directly correlated to their thermodynamic properties and the tendency to form associates in the liquid state [3]. There already exist some results of the heat capacity in the amorphous, crystalline and undercooled liquid states, obtained by differential scanning calorimetry (DSC) [4]. The composition dependence of the enthalpy of mixing of liquid lanthanum-rich alloys at 1073 K has been measured recently [5]. For a better knowledge of the temperature dependence of the thermodynamic mixing functions of the liquid Al–La–Ni alloys, the heat capacity in the stable liquid state is measured using an adiabatic calorimeter. In this paper, we present the results of the temperature dependence of C_p in the stable liquid state measured at ten different alloy compositions in the composition range of good glass formation. The results of the heat capacity of liquid aluminum and magnesium which has been measured recently [6] show that the C_p of liquid alloys can be determined from the adiabatic calorimeter without any calibration procedure. Furthermore, the association-model calculation of the liquid ternary alloys will be discussed in the light of the new $C_p(x,T)$ data. The extrapolations of the heat capacity into the undercooled melt will be presented.

2. Experimental

The heat capacity of liquid Al–La–Ni alloys was determined using an adiabatic calorimeter. Details concerning the calorimeter setup and the measurement procedure have been described previously [7]. The

*Corresponding author. Tel.: 49-711-2095162; fax: 49-711-1211280; e-mail: SOMMER@vaxwwl.mpi-stuttgart.mpg.de

0040-6031/98/$19.00
PII S0040-6031(97)00459-0

outer three-zone furnace provides a constant temperature zone in a gas-tight alumina tube which is positioned inside the furnace and which contains adiabatic shieldings and the boron nitride (BN) sample container. The cylindrical sample container has vertically drilled holes for the heating elements inside its wall. Nickel rods provide the electrical support and the suspension of the sample container. The temperature of the sample is measured and controlled by a thermocouple inside the container. The measurements are performed in the isothermal mode which keeps the surroundings at a constant temperature T during the measurements. The alloy samples are prepared from La (purity: 99.9%), Al (purity: 99.99%) and Ni (purity: 99.99%). The La samples were prepared and stored in an argon glove box. The samples are alloyed and casted under argon into a cylindrical copper mould. The cylindrical samples have a drilled blind hole for the stud of the BN container which houses the thermocouple.

The sample and the BN container are heated for a short time (2–4 s) and the associated small temperature increase ΔT (1–1.5 K) is measured within 10–20 s. Adiabatic condition is maintained within this short measurement time [7]. The product of the specific heat of container, heater and sample c_p^{CS} and their mass m^{CS} is given by

$$c_p^{CS}\left(T+\frac{\Delta T}{2}\right)m^{CS}=\frac{\Delta Q}{\Delta T}, \quad (1)$$

here, ΔQ is the electrical energy input supplied to the inner heater of the sample container. The heat capacity C_p^l of the liquid sample can be obtained from

$$C_p^l=\frac{m^{CS}c_p^{CS}-m(\mathrm{BN})c_p(\mathrm{BN})}{n}. \quad (2)$$

The product of the specific heat of container material and heater $c_p(BN)$ and their mass m(BN) is measured using a massive BN block with the dimensions of the sample container. n is the number of moles of the sample.

3. Results

The experimental results of the heat capacity measurement of liquid Al–La–Ni alloys are given in Table 1 and are shown in Figs. 1–4, respectively.

Table 1
Heat capacity of liquid Al–La–Ni alloys

T/K	C_p/(J mol^{-1} K^{-1})	T/K	C_p/(J mol^{-1} K^{-1})
$Al_{35}La_{50}Ni_{15}$			
1020	51.7	1135	48.9
1035	53.0	1150	48.2
1060	53.5	1160	46.0
1070	51.1	1170	45.3
1080	52.7	1185	48.0
1090	48.8	1200	45.1
1100	49.0	1210	45.5
1110	50.2	1260	44.1
1130	50.0		
$Al_{30}La_{50}Ni_{20}$			
980	56.8	1090	52.0
1000	55.8	1100	48.2
1010	53.6	1110	47.7
1030	53.4	1130	48.1
1040	53.1	1150	46.1
1050	51.2	1180	44.7
1060	51.4	1190	44.4
1070	50.0	1200	44.3
1080	52.9		
$Al_{20}La_{50}Ni_{30}$			
1035	58.8	1120	50.7
1050	57.3	1125	52.6
1055	58.1	1130	50.6
1060	56.6	1135	51.3
1070	56.9	1140	49.1
1080	55.8	1150	49.3
1090	54.7	1160	47.9
1095	52.7	1170	48.1
1100	52.3	1180	45.7
1110	52.0		
$Al_{13}La_{50}Ni_{37}$ (sample 1)			
1054	51.1	1213	45.8
1074	52.7	1233	47.1
1084	51.3	1253	45.5
1141	47.5	1258	44.9
1159	50.5	1273	45.1
1169	48.3	1284	43.8
1183	48.8	1298	43.2
1203	45.3		
$Al_{13}La_{50}Ni_{37}$ (sample 2)			
1064	52.3	1135	47.7
1070	52.0	1141	47.5
1074	51.0	1159	48.3
1095	48.7	1165	47.7
1100	49.6	1175	47.6
1115	50.3	1190	46.7
1125	51.2	1240	44.7

Table 1
(*continued*)

$Al_5La_{50}Ni_{45}$			
1024	48.2	1079	47.7
1029	50.9	1089	45.8
1036	52.3	1099	47.5
1039	50.2	1106	45.1
1049	49.8	1115	44.3
1054	49.2	1139	45.1
1064	48.5	1164	43.9
1069	47.3	1189	43.2
1074	47.0		
$Al_{15}La_{70}Ni_{15}$			
923	48.4	998	46.2
933	45.7	1023	44.4
948	45.4	1048	42.4
973	46.1	1073	41.9
983	45.3	1098	40.9
$Al_{15}La_{57}Ni_{28}$			
1030	51.6	1090	48.9
1035	52.1	1095	46.4
1040	50.4	1100	48.4
1045	49.4	1110	45.9
1050	50.1	1125	45.4
1055	50.7	1145	44.9
1060	50.3	1165	45.3
1065	49.7	1180	44.1
1070	47.7	1200	44.8
1075	47.5	1215	44.1
1085	50.0		
$Al_{15}La_{43}Ni_{42}$ (sample 1)			
1095	58.0	1145	56.6
1105	58.9	1155	57.4
1110	59.4	1165	54.9
1112	56.1	1180	54.1
1115	58.1	1190	51.7
1125	56.3	1215	52.1
1130	58.1		
$Al_{15}La_{43}Ni_{42}$ (sample 2)			
1105	57.7	1165	55.8
1110	56.3	1190	55.3
1115	58.4	1215	51.4
1140	55.9	1240	52.4
$Al_{15}La_{35}Ni_{50}$			
1115	50.8	1175	48.9
1120	50.7	1185	48.1
1135	49.2	1195	48.3
1143	49.1	1200	48.1
1145	48.9	1213	48.0
1155	49.7	1224	47.3
1165	48.2	1239	46.7
1171	49.1	1247	47.1

Table 1
(*continued*)

$Al_{30}La_{30}Ni_{40}$			
1110	56.1	1180	52.4
1130	54.7	1190	51.5
1135	56.6	1200	49.6
1145	55.2	1210	48.8
1150	56.2	1220	51.9
1155	54.6	1230	50.0
1160	52.6	1240	48.5
1165	52.9	1250	50.0
1170	51.1	1260	47.2

Table 2
Liquidus temperatures T_L of La-rich Al–La–Ni alloys

Alloy composition	$T_L \pm 10$/K	Alloy composition	$T_L \pm 10$/K
$Al_{35}La_{50}Ni_{15}$	1010	$Al_{15}La_{70}Ni_{15}$	920
$Al_{30}La_{50}Ni_{20}$	970	$Al_{15}La_{57}Ni_{28}$	1020
$Al_{20}La_{50}Ni_{30}$	1040	$Al_{15}La_{43}Ni_{42}$	1090
$Al_{13}La_{50}Ni_{37}$	1050	$Al_{15}La_{35}Ni_{50}$	1120
$Al_5La_{50}Ni_{45}$	1020	$Al_{30}La_{30}Ni_{40}$	1125

The standard deviation of the results is in the order of ±3%. The C_p-values at 1073 K are shown in the composition triangle as interpolated isoheat capacity lines in Fig. 5. Table 2 presents the liquidus temperatures of La-rich Al–La–Ni alloys. These were determined from the C_p-measurements using the fact that C_p of a crystalline solid has lower value than that of the liquid phase. This can be exemplified for the alloy $Al_{30}La_{50}Ni_{20}$ with: (C_p^s(700 K)=29.5 J mol^{-1} K^{-1} [4] and C_p^l (1023 K)=53.0 J mol^{-1} K^{-1}). The crystallization of a solid phase at $T<T_L$ causes a reduction of the total heat capacity of the sample. Therefore, T_L can be identified as a jog in the $C_p(T)$-curve and can be determined with an accuracy of ca. ±10 K. The T_L-values obtained from the C_p^l-measurements are very low in comparison to the melting temperatures T_m of intermetallic phases of the limiting binary systems. This effect is most significant for the Al–La and La–Ni systems. Though the ternary intermetallic phases are reported for Ni– and Al-rich Al–La–Ni alloys [8] but for the composition range examined here there is no information about the phase equilibria. Due to the relatively small temperature difference between T_L and the glass transition temperature T_g, the lanthanum rich liquid Al–La–Ni alloys can be easily quenched into the glassy state [1].

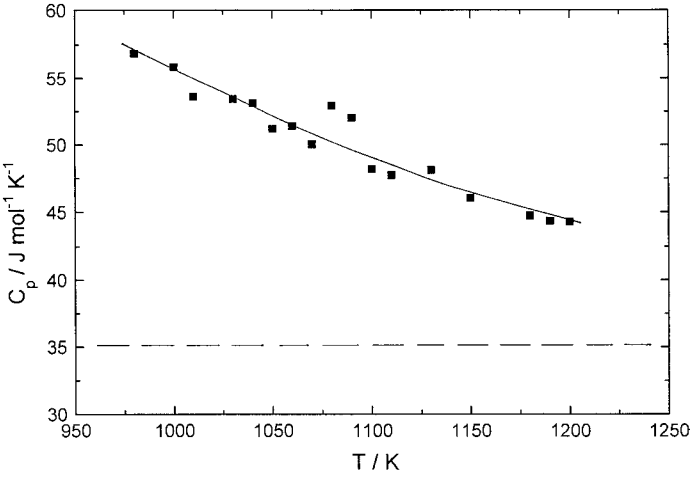

Fig. 1. Heat capacity of the liquid $Al_{30}L_{50}Ni_{20}$ alloy. (- - -) Heat capacity of the mechanical mixture of the liquid or undercooled liquid components.

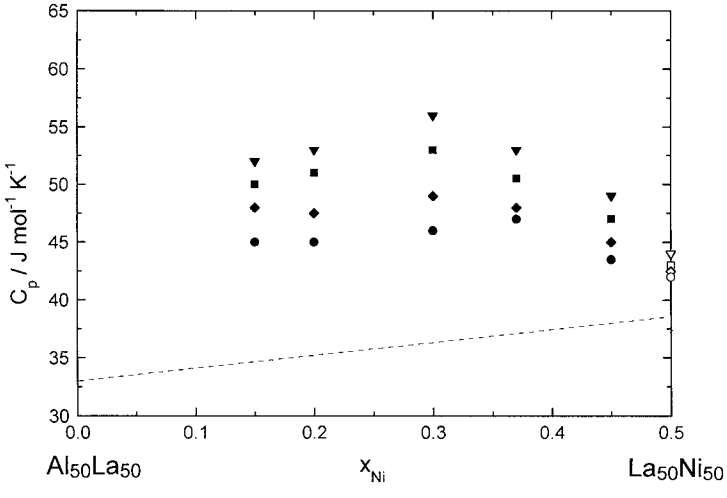

Fig. 2. Heat capacity of liquid $Al_{50}La_{50}$–$La_{50}Ni_{50}$ alloys. (▼) 1050 K, (■) 1100 K, (◆) 1150 K and (●) 1200 K, (- - -) Heat capacity of the mechanical mixture of the liquid or undercooled liquid components; (▽),(□),(◇) and (○) [5].

4. Discussion

The C_p of the liquid Al–La–Ni alloys exhibit large values and a strong temperature dependence (Fig. 6). The excess heat capacity ΔC_p^l is given by the difference between the measured heat capacity of the liquid alloy and the mechanical mixture of the heat capacities of the pure liquid components. The $C_{p,i}^l(T)$ of the pure components in the liquid and undercooled liquid state was calculated using known C_p^l-values at their melting temperatures [9], assuming constant values in the entire temperature range,

$$C_p^l(x,T) = \Delta C_p^l(x,T) + \sum_{i=1}^{3} x_i C_{p,i}^l(T). \qquad (3)$$

The values for $\Delta C_p^l(x,T)$ are shown in Figs. 7–9. The excess heat capacity and its temperature dependence is large in comparison to the results of the limiting binary systems. The maximum ΔC_p and C_p values center

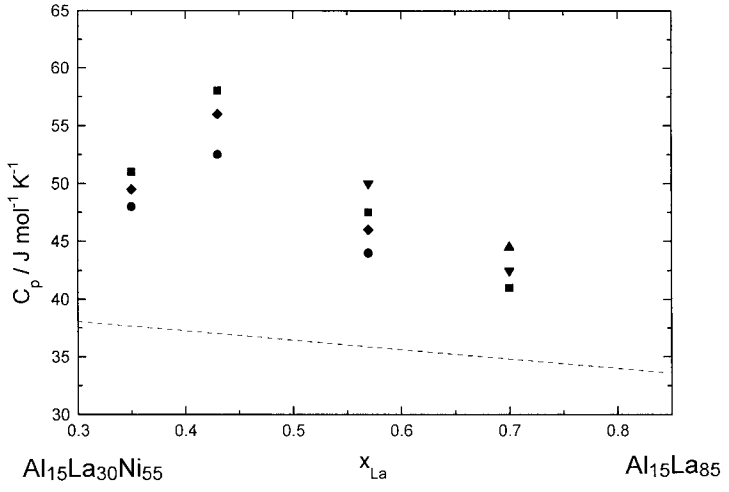

Fig. 3. Heat capacity of liquid $Al_{15}La_{30}Ni_{55}$–$Al_{15}La_{85}$ alloys. (▲) 1000 K, (▼) 1050 K, (■) 1100 K, (◆) 1150 K, and (●) 1200 K. (- - -) Heat capacity of the mechanical mixture of the liquid or undercooled liquid components.

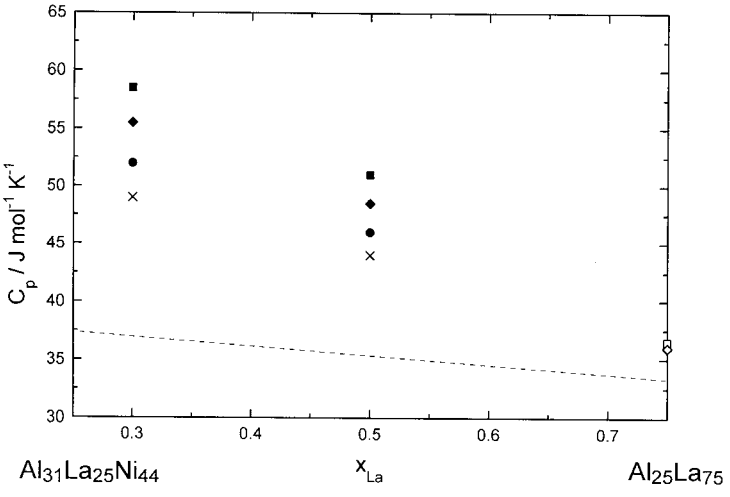

Fig. 4. Heat capacity of liquid $Al_{31}La_{25}Ni_{44}$–$Al_{25}La_{75}$ alloys. (■) 1100 K, (◆) 1150 K, (●) 1200 K, and (×) 1250 K. (- - -) Heat capacity of the mechanical mixture of the liquid or undercooled liquid components; (□) and (◇) [5].

around the composition $Al_{25}La_{37}Ni_{38}$ (Figs. 2–5 and Figs. 7–9). There exists a systematic temperature and composition dependence of C_p^l with maximum values of ca. 55 J mol^{-1} K^{-1} close to $Al_{25}La_{37}Ni_{38}$ at 1073 K.

The C_p values of the good glass-forming liquid $Al_{30}La_{50}Ni_{20}$ alloy are shown in Fig. 6 together with the heat capacity of the crystalline C_p^s and of undercooled liquid state. The value at T_L is larger than those of the undercooled liquid state above the glass-transition temperature. The C_p^l (T) curve should, therefore, exhibit a maximum in the undercooled liquid state [4]. The large C_p^l values of the liquid $Al_{30}La_{50}Ni_{20}$ alloy above T_L do not correspond to a specific behavior of this glass-forming alloy, as shown in Figs. 2–5. It has been shown [4] that the experimentally obtained C_p^l of $Al_{30}La_{50}Ni_{20}$ and their extrapolated temperature dependence of the undercooled liquid state given in

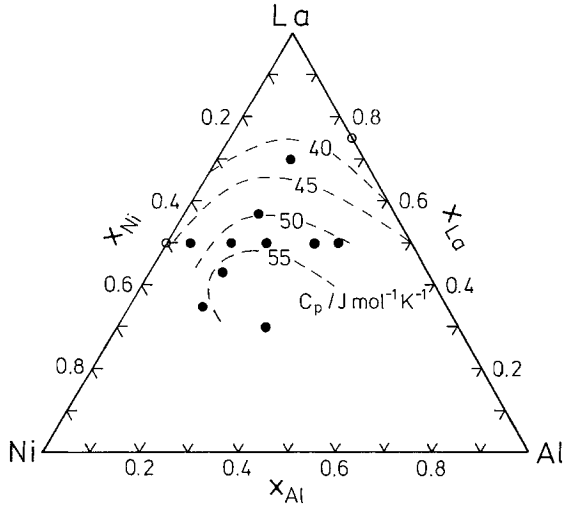

Fig. 5. Heat capacity of liquid Al–La–Ni alloys at T=1073 K. (●) measurement compositions and (○) [5]).

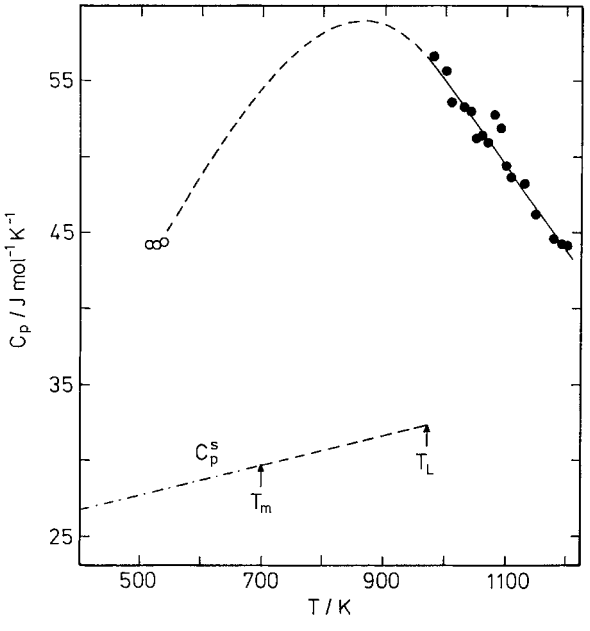

Fig. 6. Heat capacity of (●) liquid, (○ [4]) undercooled liquid and (– · – [4]) crystalline $Al_{30}La_{50}Ni_{20}$ alloy.

Fig. 6 agree with the thermodynamic relation

$$-\Delta H^{c}(T_c) = \Delta H^{m}(T_m) + \Delta H^{*} \quad (4)$$

with

$$\Delta H^{*} = \int_{T_m}^{T_c} (C_p^{l} - C_p^{s}) dT \quad (5)$$

where the heat capacity of crystalline and undercooled liquid $Al_{30}La_{50}Ni_{20}$ and the crystallization enthalpy (ΔH^{c}) and temperature (T_c) were obtained by DSC [4]. The enthalpy of melting ΔH^{m} of this alloy was measured by DTA [4].

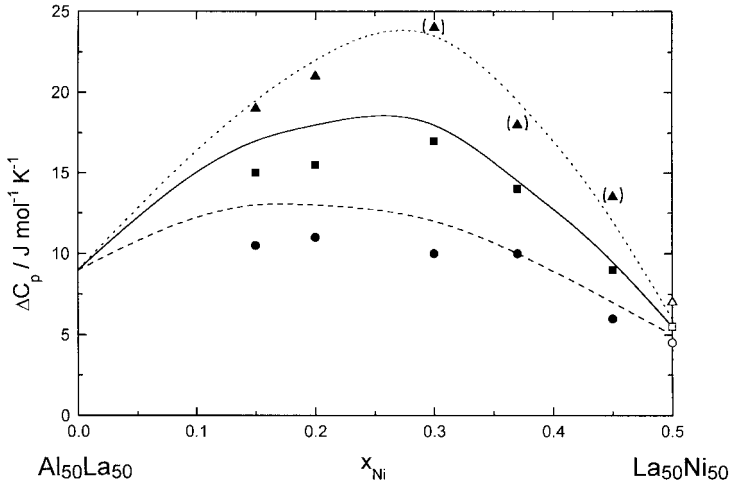

Fig. 7. The excess heat capacity of liquid $Al_{50}La_{50}$–$La_{50}Ni_{50}$ alloys. (▲) 1000 K, (▲) extrapolated value, (■) 1100 K, (●) 1200 K; (- - -) 1000 K, (———) 1100 K, and (– – –) 1200 K, calculated using the association model; (△),(□),(○) [5]).

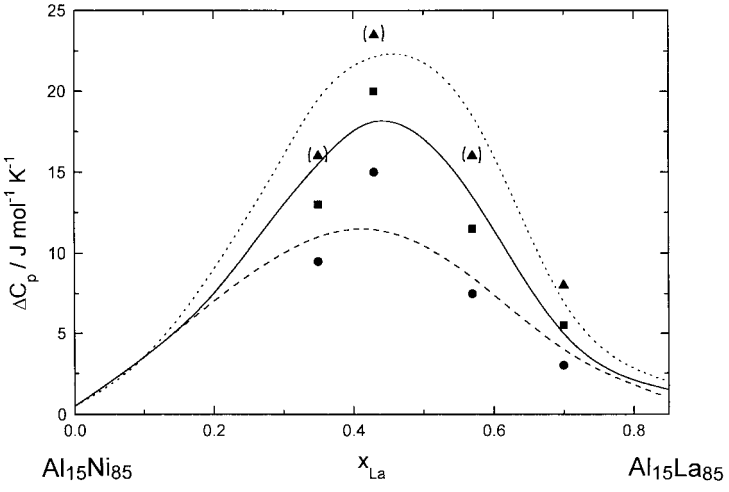

Fig. 8. The excess heat capacity of liquid $Al_{15}Ni_{85}$-$Al_{15}La_{85}$ alloys. (▲) 1000 K, (▲) extrapolated value, (■) 1100 K, and (●) 1200 K; (- - -), 1000 K, (———) 1100 K, (– – –) 1200 K calculated using the association model).

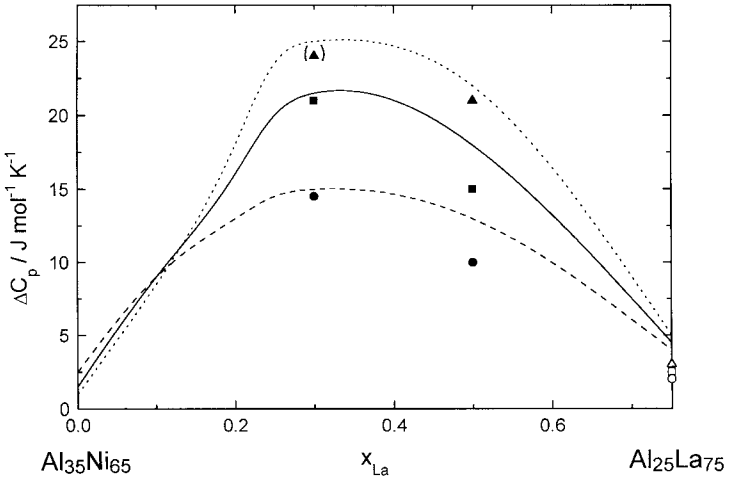

Fig. 9. The excess heat capacity of liquid $Al_{35}Ni_{65}$–$Al_{25}La_{75}$ alloys. (▲) 1000 K, (▲) extrapolated value, (■) 1100 K, and (●) 1200 K; (- - -, 1000 K, (———) 1100 K, (– – –) 1200 K calculated using the association model; (△),(□),(○) [5]).

5. Calculation of the thermodynamic properties of liquid and undercooled liquid Al–La–Ni alloys

Chemical short-range order (CSRO) occurs in the alloy melts with strong compound-forming tendency. The CSRO depends on composition and temperature. The association model given by Sommer [10] describes the relation between CSRO and the thermodynamic mixing functions. The model assumes the existence of associates, each with defined stoichiometry but undefined lifetime and free atoms in dynamic equilibrium with them. This equilibrium is governed by the law of mass action. The composition of these associates is often similar to that of corresponding intermetallic compounds. For binary and higher component (j>2), liquid alloys the following relations hold

[11] for the enthalpy and entropy of mixing,

$$\Delta H = \frac{1}{\sum_{j=1}^{k} n_j} \times \left(\frac{1}{2} \sum_{k=1}^{k'} \sum_{l=1}^{k'} C_{k,l}^{\mathrm{reg}} \frac{n'_k n'_l}{\sum_{i=1}^{k'} n'_i} + \sum_{i=1}^{k'} n'_i \Delta H_i^0 \right), \tag{6}$$

$$\Delta S = \frac{1}{\sum_{j=1}^{k} n_j} \left(-R \sum_{i=1}^{k'} (n'_i \ln z_i + n'_i \Delta S_i^0) \right), \tag{7}$$

where k is the number of components, n the number of moles of the components, k' the number of species (monomer, associates), n'_i the number of moles and z the composition of the species, respectively. ΔH_i^0 and ΔS_i^0 are the enthalpy and entropy of formation of the associates with $\Delta G_i^0 = \Delta H_i^0 - T\Delta S_i^0 < 0$. The monomers (say A) are described as associates of the type $A,B_0,C_0,\ldots$ and the Gibbs energy of formation $\Delta G_{A,B_0,C_0}^0 = 0$. The interaction parameters between the species k and l are represented by $C_{k,l}^{\mathrm{reg}}$ and it is assumed that $C_{k,k}^{\mathrm{reg}} = 0$. The equilibrium values of n'_i are determined by the law of mass action,

$$\exp[-(\Delta H_i^0 - T\Delta S_i^0)/RT] = \frac{z_i \gamma'_i}{\prod_{j=1}^{k} (z_j \gamma'_j)^{e_{i,j}}}, \tag{8}$$

γ' is the activity coefficient of the respective species k and $e_{i,j}$ the stoichiometric factor of component j in associate i. The parameters ΔH_i^0 and ΔS_i^0 and the interaction parameters are determined by solving Eqs. (6)–(8) iteratively by fitting the experimental data, such as ΔH, ΔC_{p} and the activities.

These parameters can be determined for liquid Al–La [12], Al–Ni [13] and La–Ni [5] alloys assuming the existence of Al_2La_1, Al_1Ni_1 and La_1Ni_2 associates, respectively. The stoichiometries Al_2La_1 and Al_1Ni_1 correspond to intermetallic compounds with the same stoichiometry. For the model description of the thermodynamic properties of the liquid La–Ni alloy, it was necessary to assume temperature-dependent $\Delta H_{\mathrm{La_1Ni_2}}^0$ – and $\Delta S_{\mathrm{La_1Ni_2}}^0$ – values [5]. The association model parameters of the basic binary systems are given in Table 3.

For the calculation of the thermodynamic properties of the ternary liquid Al–La–Ni alloys one has to consider three binary associates and the three pure components. It is assumed that the associates interact only with the free atoms but there is no interaction between the different associates themselves. The equilibrium values of the mole numbers of the different species, n'_i, are determined by laws of mass action according to Eq. (8) with the model parameters listed in Table 3.

$\Delta H(x,T)$ and $\Delta S(x,T)$ of liquid and undercooled liquid Al–La–Ni alloys were calculated according to Eqs. (6) and (7). The obtained $\Delta H(x)$-values at 1073 K are less negative than the measured values

Table 3
Association model parameters of the binary systems (in kJ mol^{-1})

Associate	Al–La Al_2La_1	Al–Ni Al_1Ni_1	La–Ni La_1Ni_2
$\Delta H_{A_iB_j}^0$	−128.2	−127.0	−108.0 +0.2462*(T−1376 K) −3.578×10^{-4}*(T^2−1376^2 K^2)/2 +1.3×10^{-7}*(T^3−1376^3 K^3)/3
$\Delta S_{A_iB_j}^0$	−0.0506	−0.0289	−0.028 +0.2462* ln(T/1376 K) −3.578×10^{-4}*(T−1376 K) +1.3×10^{-7}*(T^2−1376^2 K^2)/2
$C_{A_1,B_1}^{\mathrm{reg}}$	−98.1	−68.9	−86.0
$C_{A_1,A_iB_j}^{\mathrm{reg}}$	−50.9	−23.0	−37.0
$C_{B_1,A_iB_j}^{\mathrm{reg}}$	−86.3	−32.7	−47.0
Data used for fitting/Reference	ΔH at 1120 K and 1200 K: [12], $\Delta C_{\mathrm{p}}(T)$: [5]	ΔH at 1700 K: [13], a_{Al} at 1873 K: [15]	ΔH at 1376 K: [14], $\Delta C_{\mathrm{p}}(T)$: [5]

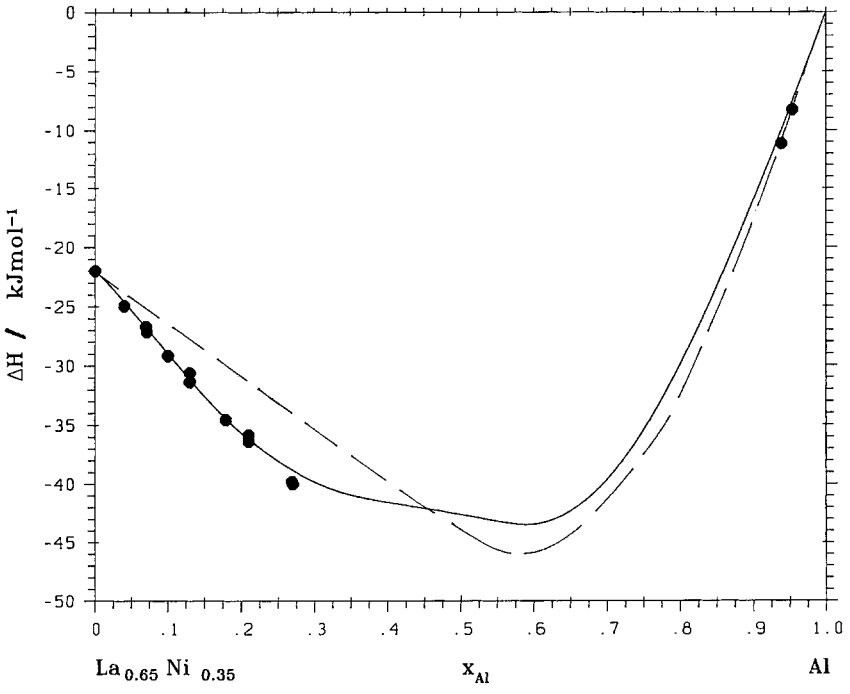

Fig. 10. Enthalpy of mixing of liquid and undercooled liquid $(La_{65}Ni_{35})_{1-x}$–Al_x alloy at 1073 K [5] calculated using the association model. (- - -) Calculation using the associates Al_2La_1, Al_1Ni_1 and La_1Ni_2; (———) calculation using the associates Al_2La_1, Al_1Ni_1, La_1Ni_2 and $Al_2La_3Ni_3$ and (●) experimental results.

[5] (see also Figs. 10 and 11). The difference between experimental as well as the extrapolated values and calculated values shows systematic deviations due to ternary interactions [5]. The deviations of ca. -5 kJ mol^{-1} between ΔH^{exp} and ΔH^{calc} center around the composition $Al_{30}La_{30}Ni_{40}$. The maxima in $C_{\mathrm{p}}^{\mathrm{l}}(x,T)$ show up near this composition (see Fig. 5).

The influence of ternary interactions is described in a further evaluation by an additional ternary association reaction with a $Al_2La_3Ni_3$ stoichiometry. The composition of the ternary $Al_2La_3Ni_3$ associate is close to the composition range of maximum deviations between ΔH^{exp} and ΔH^{calc} and of maximum $C_{\mathrm{p}}(x,T)$. It is assumed that this ternary associate interacts only with the three components but not with the three binary associates. The first set of parameters was fixed on the basis of the experimental $\Delta H(x)$ at 1073 K. The results show a good agreement to ΔH^{exp}. The excess heat capacity ΔC_p^l of liquid and the undercooled liquid ternary alloys can be obtained from the calculated dependences on temperature and composition of ΔH,

$$\Delta C_{\mathrm{p}}^{\mathrm{l}}\left(x, T_1 + \frac{T_1 - T_2}{2}\right) = \frac{\Delta H(x,T_1) - \Delta H(x,T_2)}{T_1 - T_2}. \quad (9)$$

The calculated heat capacity obtained with the first set of parameters from Eq. (9) was generally too low in comparison to the experimental $\Delta C_{\mathrm{p}}(x,T)$. Hence, it was assumed that the enthalpy and entropy of formation of the ternary $Al_2La_3Ni_3$ associate cannot be regarded as independent of temperature. If ΔH_i^0 and ΔS_i^0 are fixed at a temperature T_1, the following relationship for $T<T_1$ can be used [5]:

$$\Delta C_{p,i} = A + BT + CT^2, \quad (10)$$

$$\Delta H_i^0(T) = \Delta H_i^0(T_1) + A(T - T_1) + \frac{B}{2}(T^2 - T_1^2) + \frac{C}{3}(T^3 - T_1^3), \quad (11)$$

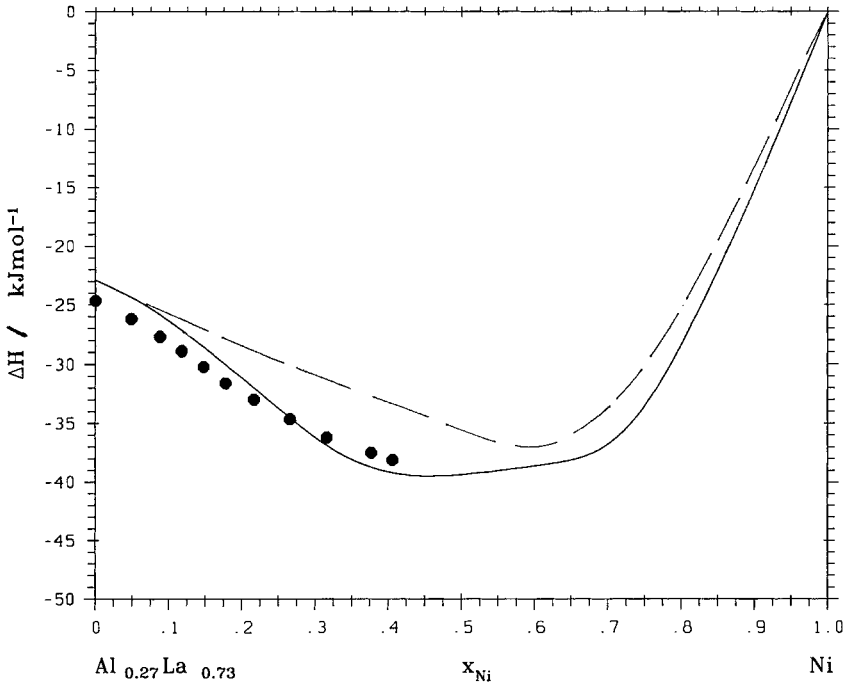

Fig. 11. Enthalpy of mixing of liquid and undercooled liquid $(Al_{27}La_{73})_{1-x}$–Ni_x alloy at 1073 K [5] calculated using the association model. (- - -) calculation using the associates Al_2La_1, Al_1Ni_1 and La_1Ni_2, (———) calculation using the associates Al_2La_1, Al_1Ni_1, La_1Ni_2 and $Al_2La_3Ni_3$; and (●) experimental results.

$$\Delta S_i^0(T) = \Delta S_i^0(T_1) + A \ln \frac{T}{T_1} + B(T - T_1) + \frac{C}{2}(T^2 - T_1^2). \quad (12)$$

A similar temperature dependence has also been assumed for the binary associate $LaNi_2$ [5] and the ternary associate $La_3Mg_4Ni_2$ [6]. The model parameters of Eqs. (6)–(8) are determined in a first step at 1300 K. In the following trial-and-error process, the temperature dependence of the formation of the ternary associate below 1300 K was fixed according to Eqs. (10)–(12) on the basis of the heat capacity data given in Table 1. The resulting model parameters are given in Table 4. The systematic deviations between ΔH^{exp} and ΔH^{calc} found by using only binary associates [5] completely vanish if the ternary association reaction with the stoichiometry $Al_2La_3Ni_3$ is assumed (see Figs. 10 and 11). The presence of ternary associates in liquid Al–La–Ni alloys results in a more negative enthalpy of mixing by ca. 5 kJ mol^{-1} near the composition $Al_{30}La_{30}Ni_{40}$. The calculated $\Delta C_p^l(x,T)$ are shown in Figs. 7–9 and are in good agreement with the experimental data within the limit of accuracy in measurement.

Table 4
Association model parameters of the ternary system (in kJ mol^{-1})

Associate	Al-La-Ni $Al_2La_3Ni_3$
$\Delta H^0_{A_iB_jC_k}$	−341.0 −0.878*(T−1200 K) +2.55×10^{-3} *(T^2−1200^2 K^2)/2 −1.44×10^{-6} *(T^3−1200^3 K^3)/3
$\Delta S^0_{A_iB_jC_k}$	−0.0012 −0.878* ln(T/1200 K) +2.55×10^{-3} *(T−1200 K) −1.44×10^{-6}*(T^2−1200^2 K^2)/2
$C^{reg}_{A_1,A_iB_jC_k}$	−40.0
$C^{reg}_{B_1,A_iB_jC_k}$	−40.0
$C^{reg}_{C_1,A_iB_jC_k}$	−40.0
Data used for fitting/Reference	ΔH at 1073 K: [5] $\Delta C_p(T)$: present study

The calculated $\Delta C_p^l(x,T)$ of liquid and undercooled liquid $Al_{30}La_{50}Ni_{20}$ shown in Fig. 12 exhibits a

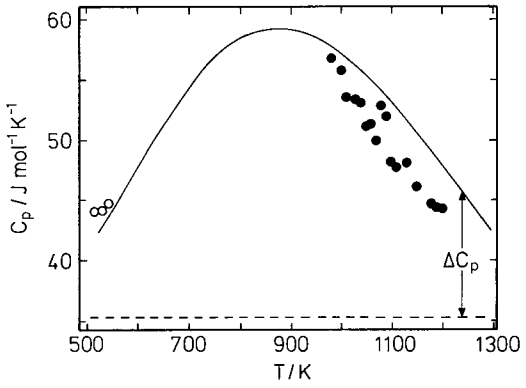

Fig. 12. Calculated ΔC_p^l of liquid and undercooled liquid $Al_{30}La_{50}Ni_{20}$ alloy. (- - -) Heat capacity of the mechanical mixture of liquid and (○) undercooled liquid components, [4].

maximum in the undercooled liquid state and corresponds reasonably to the experimental values and the extrapolated C_p^l values of Fig. 6. The temperature-dependent CSRO described with the association model, therefore, causes the maximum of $C_p^l(T)$ and their large values. The CSRO and the association tendency are generally small at high temperatures and large at low temperatures. The change in CSRO in these temperature ranges is small and, therefore, also the temperature dependence of C_p^l. The change in CSRO is large in the temperature range in-between and exhibits there a maximum. The results of the $Al_{30}La_{50}Ni_{20}$ alloys provide the experimental evidence that $C_p^l(x, T)$ of alloys exhibiting metallic bonding could show a maximum in the liquid or undercooled liquid state. The maximum in $C_p^l(T)$ of the undercooled liquid alloys can be explained within the model description by the temperature-dependent mole numbers of the assumed species. For the undercooled liquid $Al_{30}La_{50}Ni_{20}$ alloy, the mole number of the La_1Ni_2 associate decreases and the slope of the temperature dependence of the mole number of the $Al_2La_3Ni_3$ associate changes below 900 K.

6. Conclusion

The CSRO in liquid compound-forming ternary alloys can be expressed in terms of binary and ternary association reactions, where associates and free atoms are in dynamic equilibrium. The observed maximum in $C_p^l(T)$ can be explained by the temperature-dependent mole numbers of the assumed species.

References

[1] A. Inoue, M. Kohinata, A. Tsai, T. Masumoto, Mat. Trans. JIM 30 (1989) 378.
[2] P. Dantzer, J. Less-Common Met. 131 (1987) 349.
[3] F. Sommer, in: S. Steeb, H. Warlimont (Eds.), Rapidly Quenched Metals, Elsevier B.V., Amsterdam, 1985, p. 153.
[4] F. Sommer, Mater. Sci. Eng. A 226–228 (1997) 757.
[5] H. Feufel, F. Schuller, J. Schmid, F. Sommer, J. Alloys Comp. 257 (1997) 234.
[6] J. Schmid, F. Sommer, J. Alloys Comp. (1998).
[7] M. Bienzle, F. Sommer, Z. Metallkd. 85 (1994) 11.
[8] G. Petzow, G. Effenberg (Eds.), Ternary Alloys, Vol.6, VCH Weinheim, 1990.
[9] A.T. Dinsdale, CALPHAD 15 (1991) 317.
[10] F. Sommer, J. Non-Cryst. Solids 117/118 (1990) 505.
[11] H.-G. Krull, R.N. Singh, F. Sommer, to be published.
[12] F. Sommer, M. Keita, H.-G. Krull, J.J. Lee, B. Predel, J. Less-Common Met. 137 (1988) 267.
[13] U.K. Stolz, I. Arpshofen, F. Sommer, B. Predel, J. Phase Equilibria 14 (1993) 473.
[14] S. Watanabe, O.J. Kleppa, J. Chem. Thermodyn. 15 (1983) 633.
[15] F. Vachet, P. Desre, E. Bonnier, Compt. Rend. 260 (1965) 453.